

DOI: 10.1002/adma.200602221

# Universal Gradient Substrates for “Click” Biofunctionalization\*\*

By Nathan D. Gallant, Kristopher A. Lavery, Eric J. Amis, and Matthew L. Becker\*

Biomimetic surfaces are engineered to present ligands for specific receptors, thereby controlling cell–material interactions to elicit a desired response. The presentation of these bioactive ligands strongly influences the cell response, and threshold concentrations are often necessary to support adhesion or trigger signals that encourage tissue formation.<sup>[1–3]</sup> Extensive work has focused on optimizing the various aspects of ligand immobilization to enhance material-directed cell function.<sup>[4,5]</sup> Alternatively, these surface-engineering approaches can be used to design measurement or screening tools for cell response to serially manipulate immobilized biomolecules. Combinatorial methods provide useful strategies to accelerate the discovery, development, and optimization of innovative materials products.<sup>[6,7]</sup> To facilitate research on biomimetic and tissue-engineered medical products, we have developed a novel and versatile method for fabricating continuously variable concentration gradients of surface-conjugated biomolecules. This technology utilizes graded UV oxidation of self-assembled monolayers (SAMs)<sup>[8–10]</sup> and, upon further derivatization, converts the resulting carboxylate gradient into an increasing density of alkyne functionalities appropriate for “click-chemistry” surface conjugation of biomolecules.<sup>[11–13]</sup> Thus, any appropriately engineered bioactive ligand (e.g., protein or peptide) that possesses an accessible azide group can be immobilized onto the surface-concentration gradient, which we have therefore named a “Universal Gradient Substrate for Click Biofunctionalization”. The copper(I)-catalyzed Huisgen cycloaddition reaction has been highlighted recently in numerous material science applications,<sup>[12,14,15]</sup> and is proving invaluable for the facile preparation of highly func-

tional macromolecules<sup>[15–18]</sup> and the surface immobilization of biomacromolecules.<sup>[19–26]</sup> Its versatility can be directly attributed to its high degree of conversion, complete chemical specificity, and the adaptability of the reaction to numerous aqueous and mixed solvent conditions.

This combinatorial approach coupled with high-throughput analysis techniques such as automated fluorescence microscopy forms the basis of a platform for screening the ligand-density dependence of cell response to biomaterials. In the current study, this technology was used to fabricate a gradient of a glycine–arginine–glycine–aspartate–serine (GRGDS) linear peptide. Cell adhesion to adsorbed proteins or adhesive motifs engineered on surfaces is critical to biomaterials, tissue engineering, and biotechnological applications.<sup>[27]</sup> One use of this versatile technology is as a testing platform for investigating cell adhesion to surfaces functionalized with adhesive motifs derived from the native extracellular matrix (ECM). The arginine–glycine–aspartate (RGD) tripeptide sequence found in many ECM proteins is a primary binding site for cell adhesion and is recognized by a number of integrin receptors.<sup>[28,29]</sup> The design, fabrication, and characterization of an RGD cell adhesion gradient as a test application for cell response measurements to bioactive surface gradients is described.

Our approach to the fabrication of bioactive surface gradients has been to develop and characterize a functional gradient substrate to which a variety of species can be attached. First, linear gradients in surface energy were created on silicon wafers or glass slides.<sup>[8,9,30]</sup> SAMs made from *n*-octyldimethylchlorosilane were deposited onto clean oxide surfaces (Fig. 1), and the SAM-coated slides were placed on a motorized stage beneath the slit aperture of a UV lamp. A range of UV exposure times was obtained by decelerating the motion of the stage.<sup>[9]</sup> The rise in UV exposure time led to increasing amounts of ozone-derived oxidation of the *n*-octyldimethylchlorosilane SAM, generating a gradient in surface energy across the slide.<sup>[8,30]</sup> The oxidation of the terminal methyl groups of the SAM is kinetically controlled, enabling one to tailor wettability, adhesion, and electrical properties of the monolayers in a gradient or pattern by manipulating the residence time of the substrate beneath the UV lamp. The exposure-time-dependent oxidation results in numerous species being produced, including alcohols, aldehydes, and carboxylic acids, whose relative concentration profiles as a function of temporal and spatial exposure have been described previously.<sup>[8]</sup>

Surface energy gradients that ranged in advancing water contact angle from 15° to 103° were created on a single slide

[\*] Dr. M. L. Becker, Dr. N. D. Gallant, Dr. K. A. Lavery, Dr. E. J. Amis  
Polymers Division, National Institute of Standards and Technology  
100 Bureau Drive, Gaithersburg, MD 20899-8545 (USA)  
E-mail address: mlbecker@nist.gov

[\*\*] The authors gratefully acknowledge NIST/NRC Postdoctoral Fellowships (N.D.G. and K.A.L.) from the National Research Council and an IMS award from the National Institute of Standards and Technology for supporting this research. We thank Dr. Matthew J. Kipper for insightful discussions. This article, a contribution of the National Institute of Standards and Technology, is not subject to US copyright. Certain equipment and instruments or materials are identified in the paper to adequately specify the experimental details. Such identification does not imply recommendation by the National Institute of Standards and Technology, nor does it imply that the materials are necessarily the best available for the purpose. The “standard error of the mean” is the same as the “combined standard uncertainty of the mean” for the purposes of this work. Supporting Information is available online from Wiley InterScience or from the author.

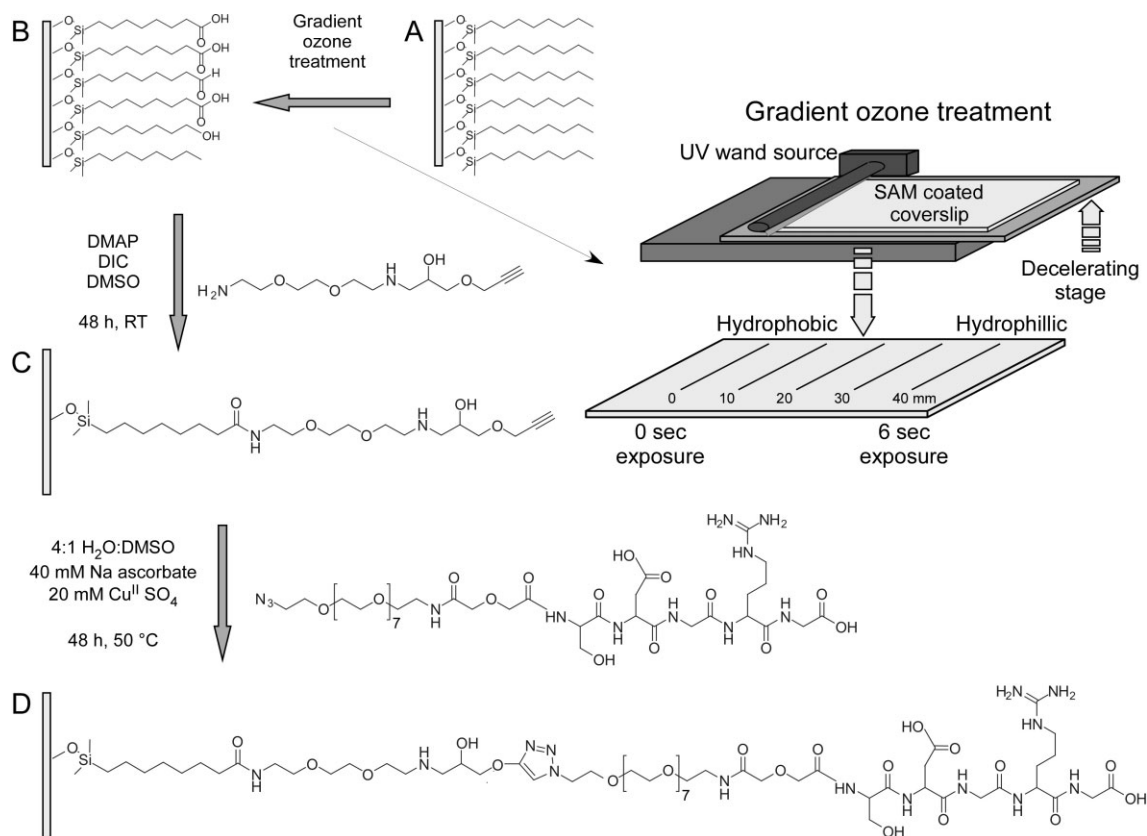


**Figure 1.** Fabrication of a Universal Gradient Substrate for Biofunctionalization, and subsequent GRGD peptide immobilization by click chemistry. A) SAMs are subjected to variable UV-ozone treatment to generate B) a monotonically increasing carboxyl density gradient. A difunctional linker converts the acid species into C) an alkyne gradient available for further biofunctionalization via click chemistry. D) An RGD azido-peptide is covalently immobilized into the gradient by triazole cycloaddition. DMAP: 4-methylaminopyridine; DIC: diisopropylcarbodiimide; DMSO: dimethylsulfoxide.

(Fig. 2A). In this instance, the prescribed conditions yielded a monotonically increasing amount of terminal acid groups in one direction. SAMs that possess surface-energy gradients have previously demonstrated their value for examining numerous physical and biological phenomena.<sup>[10,30–32]</sup> It is this concentration gradient of acid groups that forms the foundation for further functionalization and biomacromolecule immobilization. Subsequent derivatization steps preserved the monotonic change in surface energy, and similar results were observed on Si wafers and glass cover slips.

In the final fabrication step of our Universal Gradient Substrate, a bifunctional propargyl-derivatized linker was attached to the acid gradient by using standard amidation methods to yield a surface possessing an increasing concentration of alkyne groups (Fig. 1C). The propargyl gradient surface acts as a versatile substrate to which any azido-derivatized species can be attached by using click chemistry.<sup>[11,12,15,33]</sup> This reaction scheme is particularly amenable to peptide applications, because the respective functional groups are incorporated into normal synthetic schemes and neither azides nor alkynes occur naturally in amino acids ensuring desired linkage orientation.

An RGD peptide surface-concentration gradient was fabricated to assess the utility of this approach as a measurement

tool, and to investigate the dependence of RGD density on cell adhesion and spreading. Cell adhesion to RGD has been studied extensively on discrete samples;<sup>[1,34–36]</sup> however, by taking a combinatorial approach we are able to survey the cell response to a wide range of RGD densities on single-gradient substrates, and utilizing this approach affords opportunities to elucidate transition regions or other phenomena that could go undetected in a discrete format.

Many methods have been used to quantify peptide density on the surfaces of discrete samples, but standard techniques do not translate well to continuously variable gradient substrates because position and resolution are critical for mapping the local concentration. We used X-ray photoelectron spectroscopy (XPS) to measure the elemental surface concentrations as a function of position along the gradient. The nitrogen-to-carbon ratios were used to extract the fraction of alkylsilane-RGD linkages per area on the surface. Finally, from the SAM density<sup>[37]</sup> and peptide molecular mass we were able to calculate the actual immobilized peptide concentration (Fig. 2B). Because of the reproducibility of the surface-energy gradient and the efficiency of the cycloaddition reaction we expected the range of peptide densities to increase monotonically before reaching a saturation limit at the high-graft-density end, related to the availability and accessibility of reactive

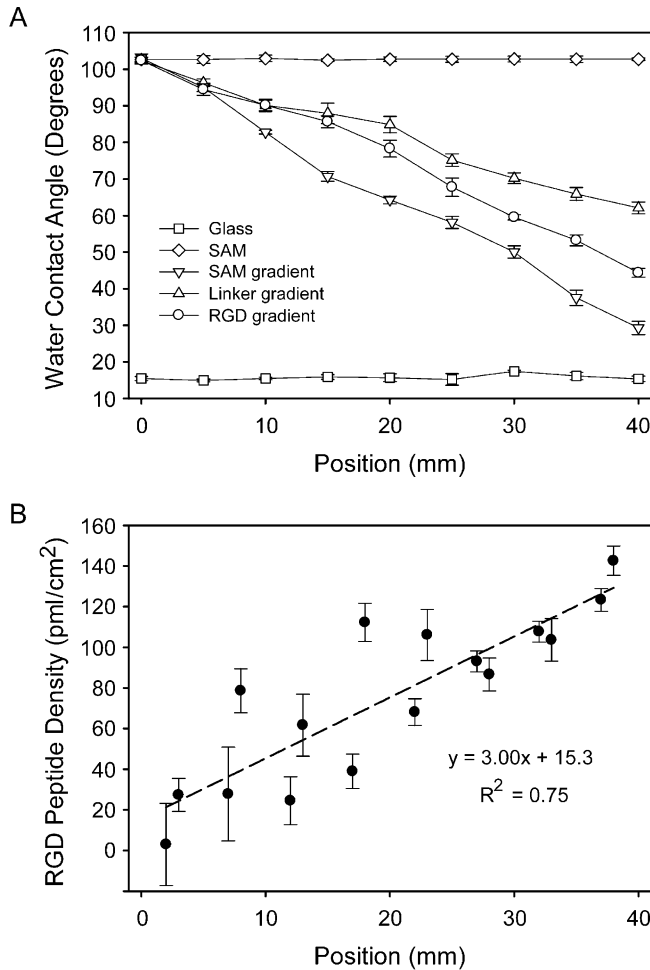


**Figure 2.** Surface energy and RGD peptide density vary as a function of position along the gradient. A) Deionized water advancing contact angle (mean  $\pm$  S.D.,  $n=6$ ) for each fabrication step depicted in Figure 1. The lines connecting the contact angle data are only used for clarity. B) Plot of the surface-conjugated RGD peptide density (mean  $\pm$  S.D.,  $n=5$ ) and its linear regression (dashed line).

sites and the size and charge of the biomolecule. However, for the given conditions the measured RGD peptide density displayed a nearly linear progression, spanning a range of approximately 0 to 140 pmol cm<sup>-2</sup>.

Smooth muscle cells (SMC) were cultured on the gradients, and automated fluorescence microscopy<sup>[30,38]</sup> was used to assess adhesion, spreading, and morphology (Fig. 3). Prior to seeding, GRGDS peptide gradient surfaces were passivated with a PEO-PPO-PEO triblock copolymer (Pluronic F68; PEO: poly(ethylene oxide), PPO: poly(propylene oxide)) and blocked with bovine serum albumin (BSA). These physisorption surface treatments were necessary to minimize nonspecific protein adsorption from serum, so the effect of the immobilized RGD on cell adhesion could be assessed. A-10 cells, a putative vascular SMC line isolated from rat thoracic aorta, were seeded (3000 cells cm<sup>-2</sup>) on gradient substrates in 2% (v/v) serum containing media and incubated for 6 h before rinsing to remove nonadherent cells, followed by fixation. The

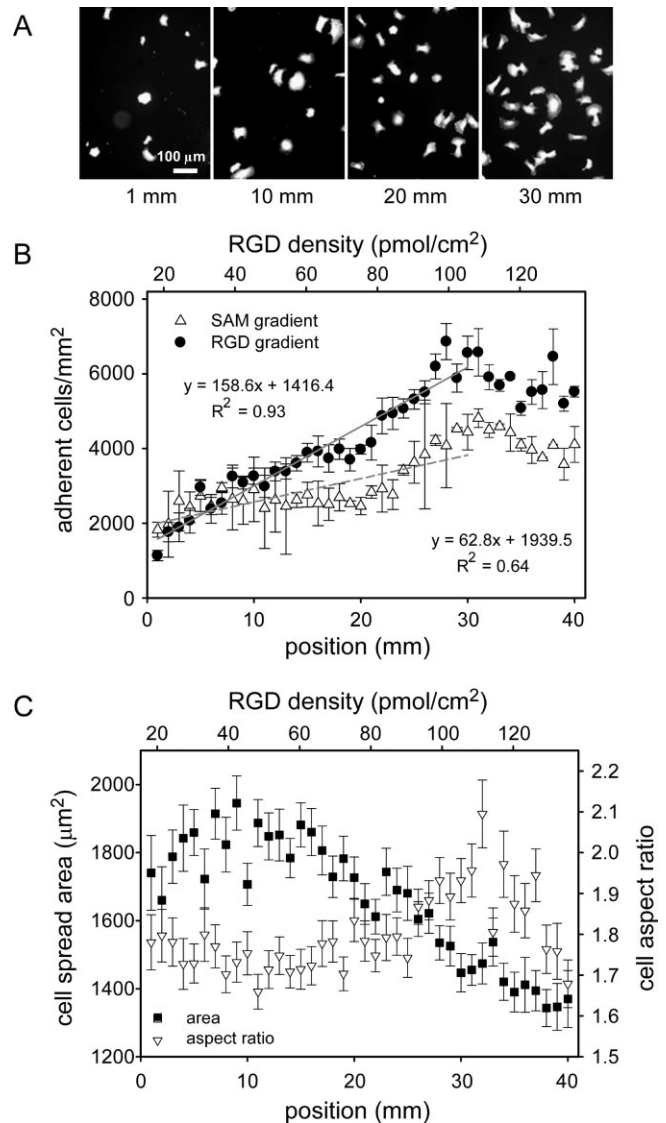


**Figure 3.** Cell adhesion and morphology vary with surface-conjugated RGD peptide density. A) Cells were fluorescently labeled, and automated microscopy combined with image analysis software was used to count the number of cells and quantify areas and aspect ratios. B) The number of cells adhering to SAM ( $\Delta$ ) or RGD ( $\bullet$ ) conjugated gradients (mean  $\pm$  S.E.,  $n=4$ ) increases with position. A second axis (top) was derived from the linear regression in Figure 2, and added to indicate cell adhesion as a function of approximate RGD density. The concentration axis (top) does not apply to the control SAM gradient ( $\Delta$ ), and the line fit equations for both peptide and control substrates are given as a function of position. C) Cell areas ( $\blacksquare$ ) and aspect ratios ( $\nabla$ , mean  $\pm$  S.E.,  $n>45$ ) versus position and RGD concentration (top axis, derived from linear regression in Fig. 2) show different trends.

number of adherent cells increased as a function of position along the gradient (Fig. 3B). The fourfold enhancement we observed correlated to the increasing RGD density of the gradient substrate. In comparison, SAM gradients without immobilized RGD exhibited an approximately twofold, but nonlinear, increase in adherent cells. This increase may be attributed to the limited ability of Pluronic to effectively

passivate nonspecific protein adsorption at the more hydrophilic end of the gradient. Cell spreading and aspect ratios exhibited opposing trends with increasing surface-bound RGD (Fig. 3C). SMC were the most spread and circular at intermediate densities (ca.  $45 \text{ pmol cm}^{-2}$ ). Interestingly, all three measured trends (adhesion, spreading, and shape) appeared to saturate beyond 30 mm, but since the underlying RGD peptide density did not reach its maximum surface concentration until 40 mm the underlying causes for the uniform cell response transitions were not obvious, and may warrant further investigation.

In summary, we demonstrate that versatile surface-density gradients can be reproducibly fabricated, and that the bioactive species of interest are easily attached via click-chemistry cycloaddition reactions. The fabrication and characterization of a Universal Gradient Substrate to which an unlimited variety of bioactive species can be attached offers a versatile platform to probe biological hypotheses where ligand concentration and orientation are important. As a first application, we have incorporated a density gradient of an adhesive RGD peptide within a nonfouling background, and observed that cell attachment was enhanced as the density of immobilized RGD increased. This demonstrates the ability to modulate a response such as cell adhesion with a bioactive peptide-functionalized gradient substrate, and is an example of the broad utility of this technology as a tool for screening surface-directed cell function. We believe that this technology for fabricating continuously variable density gradients of bioactive molecules has a wide range of potential uses in biomaterials research.

## Experimental

**Cells and Materials:** A-10 smooth muscle cells (CRL-1476, ATCC, Rockville, MD) were maintained for less than 20 passages in Dulbecco's Modified Eagle's Medium (DMEM) supplemented with 10% (v/v) fetal bovine serum (FBS), 100 units  $\text{mL}^{-1}$  penicillin, 100  $\mu\text{g mL}^{-1}$  streptomycin, and 2  $\text{mmol L}^{-1}$  L-glutamine (all from Invitrogen, Carlsbad, CA). Texas red  $\text{C}_2$ -maleimide and DAPI (4',6-diamidino-2-phenylindole) dyes were also from Invitrogen. Unless listed otherwise, all solvents and reagents were purchased from Sigma-Aldrich (St. Louis, MO) and used as received. Fmoc-protected amino acids and preloaded solid-phase Wang resins were purchased from Nova-Biochem (San Diego, CA). All glassware, stir bars, needles, reaction vessels, and syringes were oven-dried for at least 24 h, and the glassware was flame-dried under vacuum prior to use.

**Fabrication of the Universal Gradient Substrate:** Well-defined octyl dimethylsilyl (ODS) SAMs were prepared by chemical vapor deposition (CVD). Glass cover slips (24 mm  $\times$  60 mm, No 1, VWR) or silicon wafers (n-type [111], Wafer World, West Palm Beach, FL) were cleaned by air-plasma treatment (40 W, 5 min) to remove organic contaminants. The cleaned substrates were incubated in a glass desiccator under reduced pressure with octyl dimethyl chlorosilane (Gelest, Morrisville, PA) in toluene (1:4, v/v) solution at 100 °C for 72 h. Formation of complete ODS-SAMs was confirmed by the increase in advancing water contact angle from 15° to 103°. SAMs were stored under vacuum at room temperature.

Graded UV-oxidation was achieved with a computer-driven translation stage programmed to decelerate the SAM-coated substrate beneath a 190 nm UV wand-source projected through a slit aperture

(2 mm wide) cut into the lamp housing [9,30]. The ascending residence time (0 s to 6 s, 0.1 mm steps, 400 steps) of UV-ozone exposure increasingly oxidized the SAM, gradually converting the hydrophobic ( $\text{CH}_3$ -terminated) layer to hydrophilic (OH- and COOH-terminated) species [8], which could be used as initiation sites for further functionalization. Finally, the carboxyl groups were converted to acetylene functional species by the covalent attachment of a bifunctional linker (see Supporting Information). 2-Amino-2'-[(2-hydroxy ethyl propargyl ether)amino]ethylene glycol diethyl ether, was attached to the surface carboxylate groups by using standard carbodiimide chemistry (Supporting Information), yielding a substrate with a continuously variable density gradient of alkyne groups.

**Click Surface Conjugation of GRGDS Azo-Peptide:** The functional species (GRGDS-azide, Supporting Information) was attached by adding a 4:1  $\text{H}_2\text{O}:\text{DMSO}$  solution with 40  $\text{mmol L}^{-1}$  sodium ascorbate and 20  $\text{mmol L}^{-1}$   $\text{Cu}^{\text{II}}$  sulfate to a glass 15 cm petri dish containing 8 alkyne-gradient derivatized glass cover slips. This was followed by the sequential addition of the azido-derivatized peptide in DMSO. The solution was stirred for 48 h at 50 °C. The reaction solution, which turned a dark blue because of oxidation, was removed and the cover slips were washed three times each with 18  $\text{M}\Omega\text{cm H}_2\text{O}$  and ethanol, followed by drying with a nitrogen stream.

**Contact Angle Measurements:** The advancing contact angle of water on the prepared surfaces was measured at 25 °C using water as the probe fluid by operating a drop shape analysis system (DSA 10 Mr2, Krüss, Germany). The standard uncertainty of contact angle measurements at each point along the gradients was determined by the standard deviation between three independent measurements per distance on each of two samples prepared under identical conditions.

**X-Ray Photoelectron Spectroscopy:** XPS measurements were performed by using a Kratos AXIS Ultra DLD spectrometer. The employed X-ray source was monochromated aluminum, scanning over a binding-energy range of 0 to 1100 eV with a dwell time of 100 ms. Each spectrum was collected over a 300  $\mu\text{m} \times$  700  $\mu\text{m}$  sample area. The analyzer pass energy was 160 eV for the survey spectra and 40 eV for the high-resolution C1s, N1s, and O1s scans. Fits to the C, N, and O1s peaks were performed over a range of 280 to 292 eV, 396 to 404 eV, and 528 to 538 eV, respectively. Peak areas were fitted by using a Levenberg–Marquardt algorithm assuming a linear background. Based on the reaction chemistry, the expected ratios of nitrogen to carbon for each fabrication step were determined. For a given position, the fraction of total alkylsilane sites at which the functionalization and RGD linking conversion occurred within the XPS scan area was calculated by determining the local ratio of nitrogen to carbon. Finally, the extent of RGD linkage to the surface was converted to density based on the peptide molecular weight and the original alkylsilyl brush density [37].

**Automated Microscopy Measurements of Cell Adhesion and Morphology:** Prior to experiments, the A-10 vascular SMC media was changed to reduced serum (2% by volume FBS) media for 24 h. A-10 SMC were seeded (3000 cells/ $\text{cm}^2$ ) on gradient and control substrates in 2% (by volume) serum and allowed to adhere for 6 h prior to fixation and nuclear and membrane staining [38]. Cell number, cell area, and aspect ratio were determined by automated fluorescence microscopy [30] with a Leica DMR 1200 upright microscope equipped with a computer-controlled translation stage (Vashaw Scientific, Inc., Frederick, MD). Image Pro software (Media Cybernetics, Silver Spring, MD) controlled the stage and image acquisition as well as image-analysis algorithms. Gradients were imaged in a 6  $\times$  40 grid, where 6 images were collected on the axis perpendicular to the gradient and 40 images were collected at 1 mm intervals on the axis parallel to the gradient. Two fluorescence images were captured at each grid position: i) a red-channel image for Texas red  $\text{C}_2$ -maleimide-stained cell bodies, and ii) a blue channel image of DAPI-stained cell nuclei. The red cell-body images were used for determining cell area and morphology, and the blue cell-nuclei images were used to determine cell number. The aspect ratio of an object (single cell) was calculated as the ratio between the major axis and the minor axis of the ellipse equivalent of the object. Each equivalent ellipse has the same area,

first, and second degree moments as the respective object and the aspect ratio is always  $\geq 1$ . Each captured image had an area of  $0.356 \text{ mm}^2$ , and a total area of  $85.4 \text{ mm}^2$  was imaged on each gradient. Clean, untreated glass slides were used as control surfaces and scored to confirm uniform cell seeding.

Received: September 28, 2006

Revised: October 26, 2006

- 
- [1] S. P. Massia, J. A. Hubbell, *J. Cell Biol.* **1991**, *114*, 1089.
- [2] G. Maheshwari, G. Brown, D. A. Lauffenburger, A. Wells, L. G. Griffith, *J. Cell Sci.* **2000**, *113*, 1677.
- [3] C. D. Reyes, A. J. Garcia, *J. Biomed. Mater. Res. A* **2003**, *65*, 511.
- [4] R. Langer, D. A. Tirrell, *Nature* **2004**, *428*, 487.
- [5] M. P. Lutolf, J. A. Hubbell, *Nat. Biotechnol.* **2005**, *23*, 47.
- [6] E. J. Amis, *Nat. Mater.* **2004**, *3*, 83.
- [7] R. Hoogenboom, M. A. R. Meier, U. S. Schubert, *Macromol. Rapid Commun.* **2003**, *24*, 16.
- [8] S. V. Roberson, A. J. Fahey, A. Sehgal, A. Karim, *Appl. Surf. Sci.* **2002**, *200*, 150.
- [9] A. Sehgal, A. Karim, C. Stafford, M. Fasolka, *Microsc. Today* **2003**, *11*, 26.
- [10] A. P. Smith, A. Sehgal, J. F. Douglas, A. Karim, E. J. Amis, *Macromol. Rapid Commun.* **2003**, *24*, 131.
- [11] R. Huisgen, *Pure Appl. Chem.* **1989**, *61*, 613.
- [12] H. C. Kolb, M. G. Finn, K. B. Sharpless, *Angew. Chem. Int. Ed.* **2001**, *40*, 2004.
- [13] V. D. Bock, H. Hiemstra, J. H. van Maarseveen, *Eur. J. Org. Chem.* **2005**, 51.
- [14] C. J. Hawker, K. L. Wooley, *Science* **2005**, *309*, 1200.
- [15] R. K. O'Reilly, M. J. Joralemon, K. L. Wooley, C. J. Hawker, *Chem. Mater.* **2005**, *17*, 5976.
- [16] M. Malkoch, K. Schleicher, E. Drockenmuller, C. J. Hawker, T. P. Russell, P. Wu, V. V. Fokin, *Macromolecules* **2005**, *38*, 3663.
- [17] S. Srinivasachari, Y. M. Liu, G. D. Zhang, L. Prevet, T. M. Reincke, *J. Am. Chem. Soc.* **2006**, *128*, 8176.
- [18] R. J. Thibault, K. Takizawa, P. Lowenheilm, B. Helms, J. L. Mynar, J. M. J. Fréchet, C. J. Hawker, *J. Am. Chem. Soc.* **2006**, *128*, 12084.
- [19] T. S. Seo, Z. Li, H. Ruparel, J. Ju, *J. Org. Chem.* **2003**, *68*, 609.
- [20] A. J. Link, M. L. Mock, D. A. Tirrell, *Curr. Opin. Biotechnol.* **2003**, *14*, 603.
- [21] B. Parrish, R. B. Breitenkamp, T. Emrick, *J. Am. Chem. Soc.* **2005**, *127*, 7404.
- [22] M. Whiting, J. Muldoon, Y. C. Lin, S. M. Silverman, W. Lindstrom, A. J. Olson, H. C. Kolb, M. G. Finn, K. B. Sharpless, J. H. Elder, V. V. Fokin, *Angew. Chem. Int. Ed.* **2006**, *45*, 1435.
- [23] X. L. Sun, C. L. Stabler, C. S. Cazalis, E. L. Chaikof, *Bioconjugate Chem.* **2006**, *17*, 52.
- [24] M. Slater, M. Snauko, F. Svec, J. M. J. Fréchet, *Anal. Chem.* **2006**, *78*, 4969.
- [25] Y. Zhang, S. Z. Luo, Y. J. Tang, L. Yu, K. Y. Hou, J. P. Cheng, X. Q. Zeng, P. G. Wang, *Anal. Chem.* **2006**, *78*, 2001.
- [26] M. A. White, J. A. Johnson, J. T. Koberstein, N. J. Turro, *J. Am. Chem. Soc.* **2006**, *128*, 11356.
- [27] A. J. Garcia, *Biomaterials* **2005**, *26*, 7525.
- [28] E. Ruoslahti, *Annu. Rev. Cell Dev. Biol.* **1996**, *12*, 697.
- [29] S. E. D'Souza, M. H. Ginsberg, E. F. Plow, *Trends Biochem. Sci.* **1991**, *16*, 246.
- [30] S. B. Kennedy, N. R. Washburn, C. G. Simon, Jr., E. J. Amis, *Biomaterials* **2006**, *27*, 3817.
- [31] T. G. Ruardy, J. M. Schakenraad, H. C. van der Mei, H. J. Busscher, *J. Biomed. Mater. Res.* **1995**, *29*, 1415.
- [32] J. H. Lee, G. Khang, J. W. Lee, H. B. Lee, *J. Biomed. Mater. Res.* **1998**, *40*, 180.
- [33] R. Huisgen, *Proc. Chem. Soc. London* **1961**, 357.
- [34] Y. N. Danilov, R. L. Juliano, *Exp. Cell Res.* **1989**, *182*, 186.
- [35] Y. S. Lin, S. S. Wang, T. W. Chung, Y. H. Wang, S. H. Chiou, J. J. Hsu, N. K. Chou, K. H. Hsieh, S. H. Chu, *Artif. Organs* **2001**, *25*, 617.
- [36] J. Li, H. Yun, Y. Gong, N. Zhao, X. Zhang, *Biomacromolecules* **2006**, *7*, 1112.
- [37] Y. Duvault, A. Gagnaire, F. Gardies, N. Jaffrezicrenault, C. Martelet, D. Morel, J. Serpinet, J. L. Duvault, *Thin Solid Films* **1990**, *185*, 169.
- [38] C. G. Simon, Jr., N. Eidelman, S. B. Kennedy, A. Sehgal, C. A. Khatri, N. R. Washburn, *Biomaterials* **2005**, *26*, 6906.
-